MEASUREMENT OF THE HORIZONTAL COMPONENT

OF GROUND WATER FLOW USING A VERTICALLY

POSITIONED

IN-SITU THERMAL PROBE

Technical Completion Report
Project No. A-044-NMEX

MEASUREMENT OF THE HORIZONTAL COMPONENT OF GROUND WATER FLOW USING A

VERTICALLY POSITIONED IN-SITU THERMAL PROBE

Stephen G. McLin,   Graduate Research Assistant

Marshall A. Reiter,   Principal Co-Investigator,
                      Geophysicist

Allan R. Sanford,   Principal Co-Investigator,
                      Geophysicist

TECHNICAL COMPLETION REPORT

Project A-044-NMEX

ABSTRACT

A thermal probe for the in-situ measurement of groundwater flow rates in a borehole was calibrated in a vertical position. The probe is a long slender metal rod having a heat source along its entire length and a temperature sensor at its midpoint. When a constant quantity of heat is applied to the probe, the rise in temperature is inversely related to the rate of water flowing past the probe.

Full scale calibration of the probe was considered necessary because theoretical studies over-simplify the interaction between the heated probe and the horizontal flow of groundwater. The apparatus for calibration consisted of a central sand-filled chamber having a vertical hole lined with a well-screen in its center. The central chamber was hydrologically connected to upstream and downstream water reservoirs that were used to control the rate of water flowing in the central chamber.

Fifty eight calibration runs of the thermal probe were made; most of these tests were used to perfect the experimental techniques of data gathering and the design of the calibration tank. Fourteen of the calibration tests were selected to construct preliminary calibration curves. The selection of specific tests was based on a statistical analysis of the A_1 coefficients from a third order polynomial fit of the experimental data. Final calibration curves were constructed on the basis of ten calibration tests. These curves show that if a temperature difference of 0.1 degrees Centigrade can be measured at the end of a two hour test, the probe is capable of distinguishing small differences in specific discharges when the flow exceeds 120 cm/day.

ACKNOWLEDGEMENTS

TABLE OF CONTENTS

Page

LIST OF TABLES

LIST OF FIGURES

INTRODUCTION

In the evaluation of regional groundwater potential, a most important parameter is the mass rate and direction of subsurface water flow. The purpose of the present research has been to calibrate a thermal probe, in a vertical position, for the in-situ measurement of the horizontal component of groundwater flow. The probe was previously constructed and calibrated in the horizontal position (Reiter and Sanford, 1973).

The thermal probe is a long slender rod about 112 cm long and 3.8 cm in diameter. It contains a cylindrical heat source and a single temperature sensor. The probe is designed for use in boreholes and water wells. When a constant quantity of heat is supplied to the instrument, the rate of temperature increase in the probe is inversely related to the mass rate of water flowing past it. The device provides a direct method of determining the groundwater mass flow rate which is less time consuming and less expensive than today's more commonly used methods. The calibration data of the thermal probe suggest that the water mass flow rate can be determined in as little time as two hours after the probe has obtained an equilibrium temperature with its in-situ surroundings. The time required to reach equilibrium depends upon the initial difference between the temperature of the probe and the water whose rate of flow is to be determined.

One may also determine the horizontal mass rate of flow at different depths of a well, and thus at different depths of the same aquifer or of different adjacent aquifers and aquitards. The thermal probe, therefore, has many inherent advantages over other techniques for determining groundwater flow rates. However, the sensitivity of the instrument, specifically its ability to measure flow rates in the 10 cm/day range or less, will have to be improved before its use becomes widespread. Hopefully, the device may

find applicability in such engineering problems as the determination of seepage rates around dam sites, as well as regional groundwater surveys.

THEORY

The initial background theory for the use of the thermal probe as an instrument for the measurement of groundwater mass flow rates in boreholes was given by Jaeger (1940, 1956). Theoretical curves determined by a numerical integration of Jaeger's solution were given in the New Mexico WRRI Report No. 027. These curves suggest that the detection of small differences of flow rates is rather difficult. In addition Jaeger's theoretical approach does not adequately predict the response of the thermal probe. The theoretical problem assumes that water entering the boreholes is at the temperature of the surrounding sand medium, and hence the warming effect of the thermal wave from the probe is neglected. Furthermore, the theoretical model assumes that the entire borehole has the specific heat of water and the thermal conductivity of a perfect conductor.

The actual experimental situation involves the interaction of the radial flow of heat with the linear flow of water. Thus the flow pattern close to the thermal probe is complex and variable for different water flow rates. For a zero head difference across the central chamber, no water is flowing in the borehole. Thus heat is initially diffusing only radially away from the probe by conduction. An imaginary horizontal plane passing through the borehole and probe would show a symmetrical distribution of constant temperature lines, or isotherms, around the probe. The resulting curve of temperature rise in the probe versus time is approximately linear. Once convection begins, usually at about 200 seconds, there is a break in slope as heat is more rapidly transferred away from the probe.

For a non-zero head difference across the central chamber, the flow of
heat is superimposed on the linear flow of water past the probe. The imagi-
nary horizontal plane shows isotherms distributed in a tear-drop shape with
the tail pointed downstream. These isotherms also move radially outward with
time while maintaining their shape, but in a fashion depending on the mass
rate of water flowing past the probe. The resulting curves of temperature
rise versus time show the same general shape as in the zero flow case, but
the maximum temperature rise in the probe is less. In other words, the
curves are displaced downward towards the abscissa. The magnitude of the
displacement increases as the water flow rate increases. As in the case
of zero flow rates, heat is transferred away from the probe by conduction
at times less than about 200 seconds. However the heating up of the probe
eventually produces sufficient temperature gradients to trigger convection.
As a result, there is also a sharp break in these curves.

The physical processes acting around the probe are so complex that it
is unlikely that an analytical solution can be obtained. For this reason,
we elected to test the thermal probe's capabilities by full-scale calibration.

INSTRUMENTATION FOR CALIBRATION

The instrumentation is composed of three basic parts: (1) the thermal
probe, (2) the instrument panel, and (3) the calibration tank. Each will
be described separately.

(1) The thermal probe consists of two main parts, an inner core and
the outer protective sleeve (Figure 1). The inner core is a solid rod of
aluminum approximately 112 cm long and 1.1 cm in diameter. It contains the
heat source and the temperature sensor. The heat source is a glass-insulated
nichrome wire embedded in a spiral groove of two turns per 2.54 cm which has
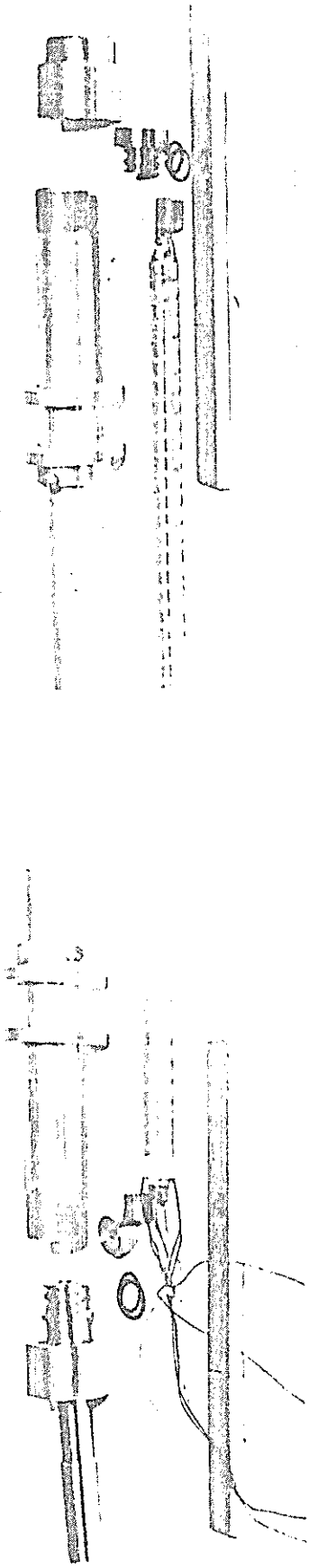
(a)
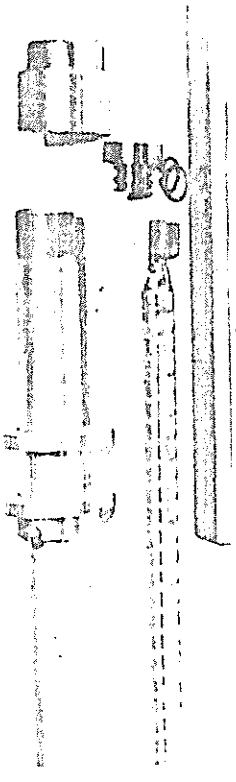
(b)
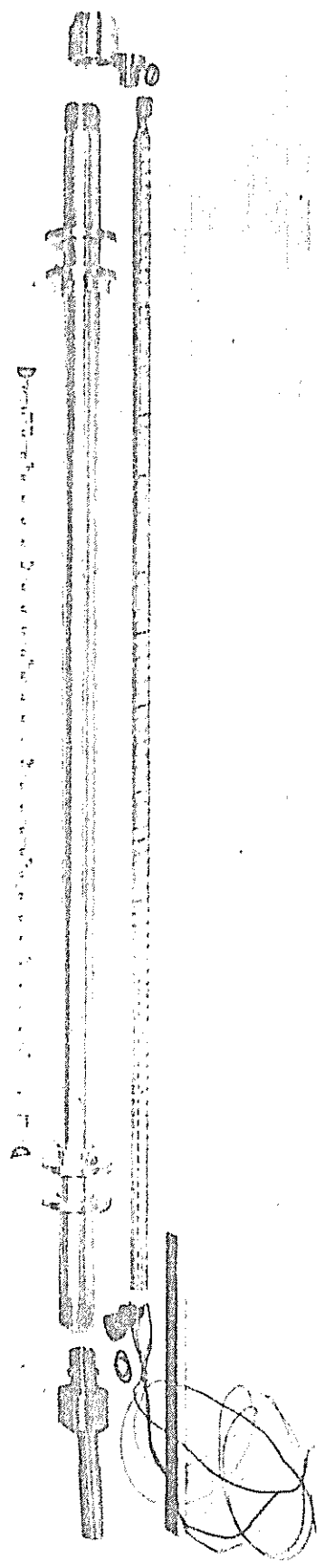
(c)

Figure 1. Thermal probe. The end of the probe that connects to the cable is shown in (a).

been machined in the rod. The total resistance of the heating element is approximately 38 ohms. A known current, passed through the heating element, serves as the heat source for the instrument. Centered midway in the rod is the temperature sensor, a thermistor having a resistance of 4,000 ohms at 25°C (Fenwall-4K-2% isocurve device).

The outer sleeve, 3.8 cm outside diameter, slides snugly over the inner core. The inner core is retained at both ends by use of bakelite wedges pressing firmly against stainless steel caps screwed over the outer sleeve. These caps are equipped with inner O-ring seals to prevent water leakage into the inner core. The heating element and the thermistor are electrically connected to a six conductor cable through the outer stainless steel fitting at the top of the probe. A stress member in the cable is secured by another connector between the inner core and the outer fitting. The outer fitting is volcanized to the cable to insure against water leakage into the inner core.

Four convection seals are secured to the outside of the probe sleeve, two at each end, by means of stainless steel rings held in place with set screws. These seals are one-half inch thick impermeable foam rubber cut with a diameter approximately one inch larger than the well screen, thus forming an oversize fit. The convection seals prevent water movement up and down in the borehole.

(2) The instrument panel consists of two main parts (Figure 2), the temperature monitoring system and the DC power supply to the heating element. A Wheatstone bridge is located in the instrument panel and is coupled with the thermistor located in the inner core of the probe. It thus provides a resistance thermometry device. The bridge and probe were constructed at New Mexico Tech and were used on earlier work (Reiter and Sanford, 1973) as
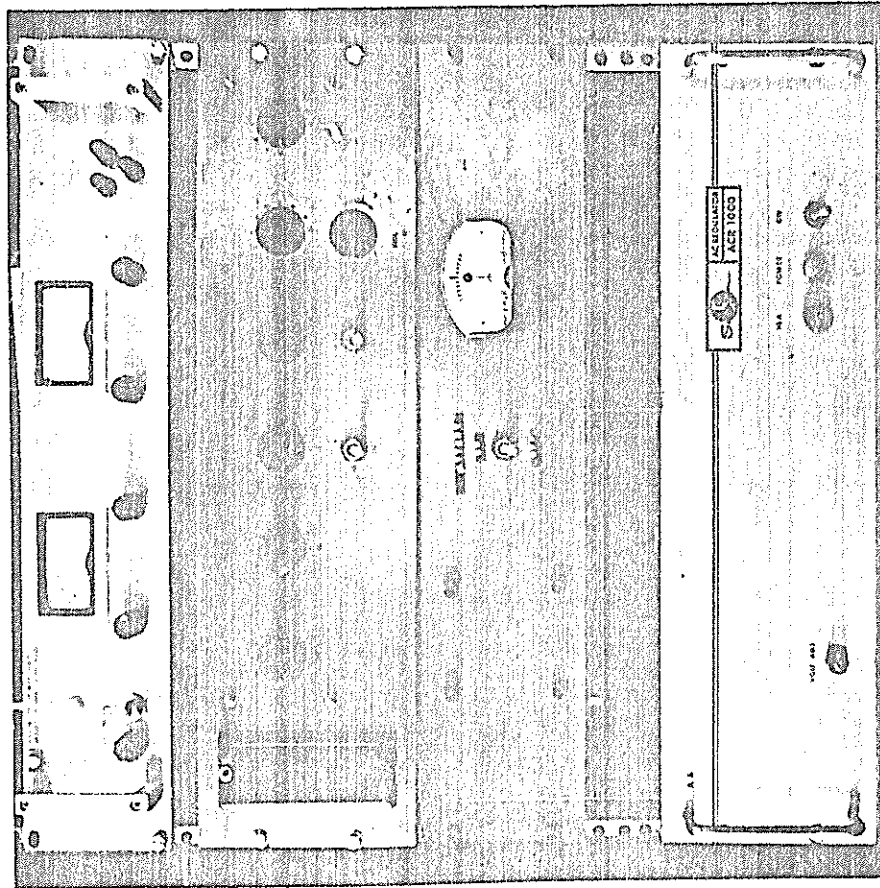
Figure 2   Instrumentation panel; probe power supply above, temperature monitoring system in middle.

well as on the present research. The bridge has a range from 0 to 100,000 ohms; however, the typical operating range with the 4K isocurve thermistor is between 5200 ohms and 2100 ohms (18°C to 43°C). The relative accuracy of the system is probably better than ±2 ohms (about ±0.01°C).

The power supply is a Hewlett-Packard SCR-1P series, model 6443B. It is a solid state constant voltage/constant current DC power supply with a variable continouous output between 0 and 120 vdc, and between 0 and 2.5 amperes. Two front panel meters provide for monitoring output voltage and current. Each meter has a 2% accuracy at full scale.

(3) The calibration tank shown in Figure 3 is welded three-eights inch thick steel plates, reinforced with an outside frame made of angle iron. The tank rests on four welded steel rails running the width of the tank. These rails provide a three inch ground clearance on the tank bottom for easy move-ment with a forklift. The tank has upstream and downstream reservoirs and a central chamber filled with sand. The inside volume of this central cham-ber is 183 cm x 183 cm x 183 cm, with a 147 cm long Johnson well screen cen-tered inside the central chamber (see Figure 4). The vertical well screen allows for the insertion and withdrawal of the thermal probe. The well screen has 0.0025 cm wide slits at 0.154 cm spacings over 142 of its 147 cm overall length. The screen is placed in the central chamber of the tank such that the geometric centers of the tank, well screen, and thermal probe all coin-cide during a calibration test.

The central chamber is hydrologically connected to the upstream and down-stream reservoirs by a steel partition of horizontally parallel gratings. In addition, an 18 by 16 fine mesh, 0.028 cm diameter screen is secured to the inside of the metal grating to prevent sand spillage into the reservoir tanks.

Figure 3   Calibration tank with probe partially inserted.

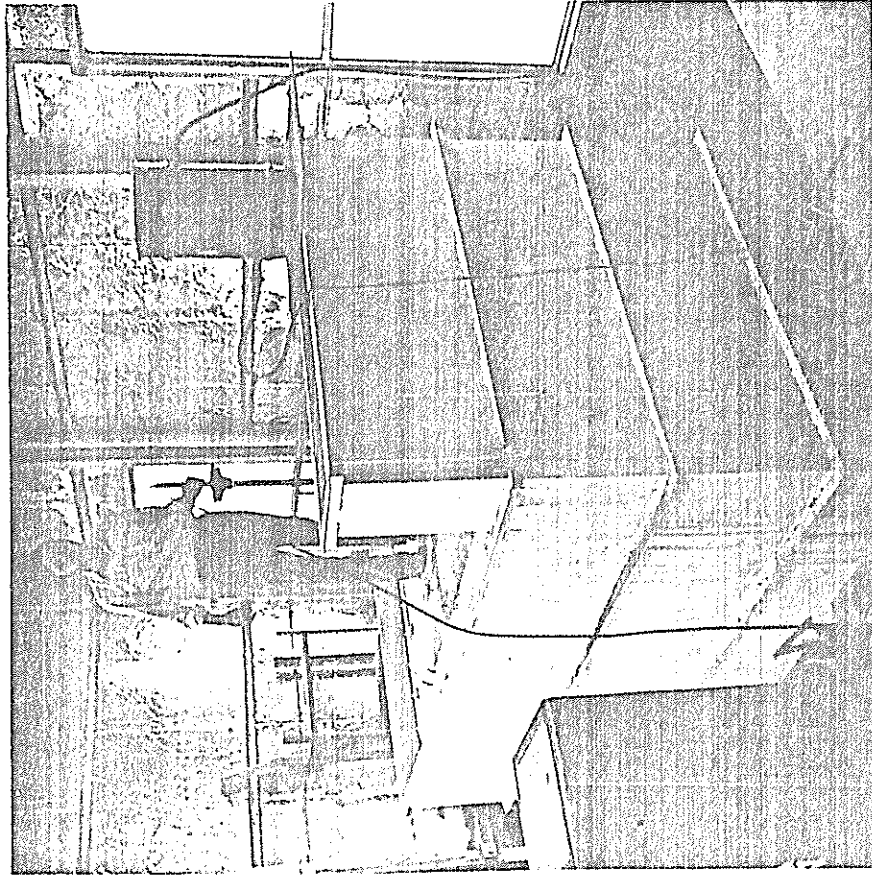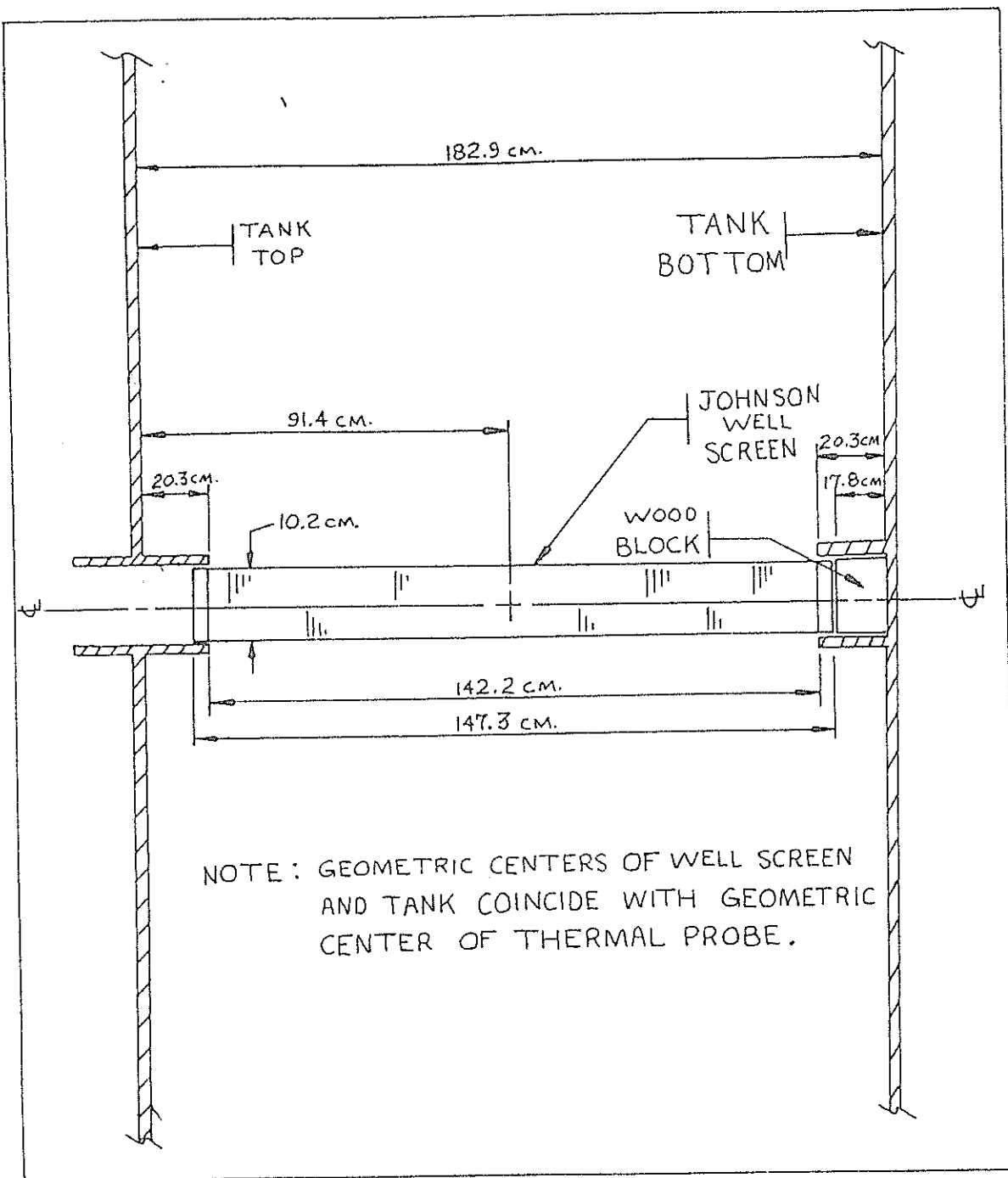Figure 4. Sketch showing critical dimensions of the central chamber and the locations of the well screen in the middle.

The two reservoir tanks hold excess water such that the head differences between them can be regulated in order to vary the hydraulic gradient acting on the sand porous medium. The head difference is controlled by a small 22 gallon drum placed on top of the upstream reservoir. Water is pumped from the downstream reservoir into the drum. An overflow line returns excess water directly to the downstream reservoir, thus maintaining a constant head of ±2 cm in the drum. A small gate valve controls the volume of water flowing from the drum into the upstream reservoir such that constant head differences to within ±0.1 cm can be maintained between the upstream and downstream reservoirs. This eliminates the need for control switches turning the pumps on or off in order to maintain a constant head across the central chamber. In addition, minor fluctuations in head are eliminated from the constant on-off cycle of the pumps. Because the system used remains closed, new water does not need to be added.

EXPERIMENTAL PROCEDURE

The method for reliable calibration of the thermal probe was as follows:

(1) The thermal probe and the water in the calibration tank were allowed to come to the same temperature. Equilibrium was assumed when the temperature of the probe, found from the resistance of the thermistor embedded in the probe, agreed to within 2°C of the temperature of the water. Normally the probe and the water were near the same temperature whenever an experiment was about to be conducted because the pumps that controlled the flow of water in the calibration tank were allowed to operate continuously. If the pumps were turned off between experimental runs, the time required for the probe and water to equilibriate was longer. This time depended upon the initial temperature difference between the probe and water, and upon the water flow rate for a particular experimental run.

Another technique was also used to further ensure temperature equili-
brium between the probe and water. Here the probe thermistor resistance
was monitored at least twenty minutes prior to a given test run. If the
thermistor resistance did not change during this period, it was assumed that
the probe temperature was very nearly the same as the water temperature.

(2) After equilibrium was established between the temperatures of the
probe and the water in the calibration tank, the mass rate of water flowing
past the probe was determined. By maintaining a constant head difference
between the upstream and downstream reservoir tanks, a constant mass rate
of flowing water, or specific discharge, was obtained. A known volume of
water was collected in the downstream reservoir over a known time interval
and the specific discharge was easily calculated from the equation

$$q_x = \frac{V}{At} \qquad , \qquad (1)$$

where q_x = horizontal component of specific discharge $(\frac{cm}{sec})$,

V = volume of water collected (cm^3),

A = cross-sectional area perpendicular to the flow direction (cm^2),

t = time interval over which V was collected (seconds).

The determination of the specific discharge for each calibration test
is, however, very time consuming. If the hydraulic conductivity is known
for the porous medium in the tank, the specific discharge can be easily
calculated knowing Δh and Δx, since the specific discharge vector is related
to the head difference by Darcy's Law. Thus

$$q_x = - K_x \frac{\Delta h}{\Delta x} \quad , \qquad (2)$$

where K_x = horizontal component of hydraulic conductivity ,

Δh = constant head difference in cm of water,

Δx = horizontal length of the flow path in the calibration tank.

The negative sign in equation (2) indicates that flow is from regions of higher to lower hydraulic head. Equation (2) is valid only for laminar flow where the Reynolds number is less than about ten. For most flows in porous media the Reynolds number is usually less than one. The Reynolds number is defined as the ratio of inertia to viscous forces. Thus a low value for this ratio indicates that viscous forces predominate and the flow is laminar. In the calibration experiments for water near 20°C, a mean grain diameter of 0.051 cm, and a maximum specific discharge of 500 cm/day, the Reynolds number is found to be approximately 0.3. Thus the flow is clearly laminar in the porous medium of the central chamber. As water enters the well screen, its velocity will approximately double as predicted from potential flow theory, still giving a Reynolds number less than unity. It therefore seems safe to assume laminar flow inside the well bore. It should be pointed out, however, that the interference effects of the well screen have been neglected in the determination of the Reynolds number inside the borehole.

If q_x, Δh, and Δx are all known, the hydraulic conductivity of the porous medium can be determined from equation (2). However, K_x, is not only dependent upon properties of the porous medium, but also upon the fluid. Thus K_x is given by:

$$K_x = \frac{k\rho g}{\mu} = \frac{k\gamma}{\mu} \qquad (3)$$

where   k = porous medium intrinsic permeability (L^2),

   ρ = fluid density (ML^{-3}),

   μ = fluid dynamic viscosity ($FL^{-2}T$),

   γ = fluid specific weight (FL^{-3}).

The intrinsic permeability depends only on the porous medium properties while the dynamic viscosity and specific weight are temperature dependent.

A standard hydraulic conductivity, K_s, can be defined as the flow of a known volume of water at 15.6°C through a porous medium of unit cross-sectional area under a unit hydraulic gradient. The field hydraulic conductivity, K_f, can be similarily defined at the field temperature. By taking the ratio of the two, only the effects of temperature are observed. In equation form this becomes:

$$\frac{K_s}{K_f} = \frac{k\gamma_s/\mu_s}{k\gamma_f/\mu_f} = \frac{\mu_f\gamma_s}{\mu_s\gamma_f} = \frac{\rho_f\nu_f\gamma_s}{\rho_s\nu_s\gamma_f} \quad . \tag{4}$$

ν = fluid kinematic viscosity $(L^2 T^{-1})$.

For a field temperature range of 0°C to 27°C, there is less than a 0.5 percent variation in the density and kinematic viscosity of water. The actual water temperature range in all of the probe calibration tests was between 18°C and 26°C. Therefore the above variation was even less for the experiments. The water temperature variation for any given probe calibration test never exceeded 0.1°C. For practical purposes then, ρ_f and ρ_s can be considered equal, as can γ_f and γ_s. Thus

$$K_s = K_f(\frac{\nu_f}{\nu_s}) \text{ , or } K_f = K_s (\frac{\nu_s}{\nu_f}) \quad . \tag{5}$$

In order to determine K_s for the porous medium in the calibration tank, eleven individual tests were run maintaining Δh constant for each. A known volume of water, V, was collected over a time interval, t, while the water temperature was monitored at the start, middle, and end of each test. At the measured water temperatures standard tables were used to determine the kinematic viscosity of the water. The corresponding field hydraulic conductivity, K_f, was found from equation (2) for each of the eleven tests. Using equation (5), each of these field values of K was translated into a standard K_s for the porous medium. The mean value of the standard hydraulic conductivity found on the eleven tests was 0.103

cm/sec. The first order polynomial fit of the same data showed a

K_s of 0.104 cm/sec., with a correlation coefficient of 0.997. A

plot of this date is shown in Figure 5.

During an individual calibration test of the probe, a constant

Δh was maintained while the water temperature was monitored at the

start, middle, and end of each run. From equation (2) the specific

discharge was calculated since K_s, Δh, and Δx were known. However

the calibration test water temperature was never exactly at 15.6°C

and caused a slight error in q as found from equation (2). By using

equation (5) first, the field hydraulic conductivity at the calibration

test water temperature was found since K_s was already known. Thus K_f

from equation (5) was used in equation (2) in place of K_s. The specific

discharge at the test water temperature was thus computed for the Δh of

an individual calibration run for the probe.

3) The procedure during an experimental run was first to record

the resistance of the bridge at the equilibrium temperature for time zero.

The resistance of the bridge was then lowered by 200 ohms. Power to the

heating element was turned on and the time and new resistance was recorded

when the bridge null-detector again read zero. The resistance was lowered

once more and the procedure repeated. During the first minute after the

power was activated, five or six readings were taken in 200 ohm increments.

As time increased the resistance increments were made progressively smaller

while the time increments increased. At 1200 seconds the bridge resistance

at a zero null-detector reading was recorded. Succeeding time increments

were then kept at a constant 300 seconds. At the end of each time interval,

SPECIFIC DISCHARGE AT 15.6 DEGREES C VS. HORIZONTAL GRADIENT OF HEAD

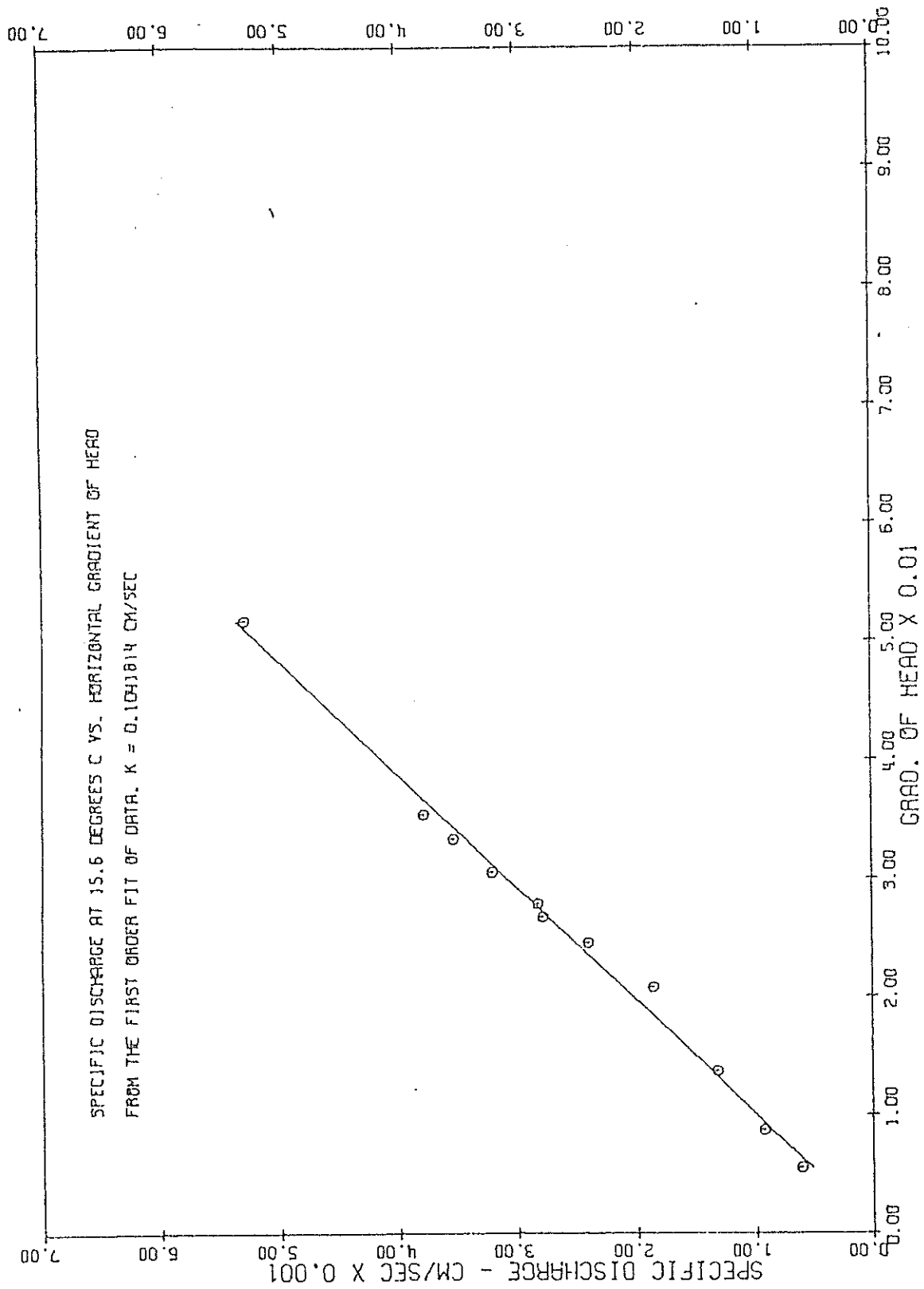FROM THE FIRST ORDER FIT OF DATA. K = 0.1041814 CM/SEC

Figure 5 Specific discharge at 15.6°C versus the gradient of head for the porous medium in the central chamber.

the resistance was recorded until the completion of the experiment
was reached at 7200 seconds. An average test consisted of from 25 to
35 of these readings over the two hour period.

Because of the difficulty in estimating the amount of time required
for the null-detector to come to zero for each reading, the bridge was
left on during the entire experiment. The effect of self-heating on
thermistor readings was previously examined (Reiter and Sanford, 1973)
and it was determined that the bridge current was too small to initiate
self-heating of the thermistor.

A Hewlett-Packard DC power supply, Series SCR-1P, model 6443P,
was used to supply a constant power to the probe heating element. Through-
out all of the calibration runs, constant voltages and currents were
maintained at 104 volts and 2.4 amps respectively. The change in power
to the probe from the start to the finish of each test was much less than
1%, according to the DC power supply specifications.

After the completion of a calibration test, the recorded times at
1200 seconds and above, and their respective resistances were punched
on computer cards. A computer program changed the recorded resistances
to temperatures in degrees Centigrade, and plotted a third order polynomial
data fit of the temperature rise as a function of time. In addition each
data deck also contained a computer card giving the head and water tempera-
ture so that the specific discharge was also calculated for each calibration
run. This procedure was repeated for various flow rates in the porous medium,
allowing one to acquire a set of calibration curves for the temperature rise
in the probe versus time.

(5) The pumps controlling the flow rate of water in the central chamber of the calibration tank were allowed to operate continuously. They were shut off only when necessary; that is, when a calibration test involving zero flow rate was made, or when repairs on the equipment were required. By keeping water continually circulating in the tank, one could be sure that the sand in the central chamber remained fully saturated. In addition the effects of temperature fluctuations in the water arising from diurnal variations in room temperature were somewhat reduced by continuous circulation through the tank.

PRESENTATION AND DISCUSSION OF CALIBRATION DATA

The data obtained during the calibration of the thermal probe are presented in Tables 1 and 2 and Figures 7 through 13. Table 3 explains the headings used in Tables 1 and 2. Figures 7, 8, 9, 11 and 12 show plots of the probe temperature rise versus time for different water flow rates. Figures 10 and 13 show maximum temperature rise in the probe versus the specific discharge for each test. The calibration test numbers are given in each plot for cross-reference to the tables.

All results presented in this report are from calibration tests in a screened borehole. The borehole is lined with a 10.16 cm diameter Johnson well screen having 0.0025 cm wide slots at 0.154 cm spacings over 142 of its 147 cm overall length.

General Characteristics of Curves

Characteristic test data are shown in Figure 6 over the entire data range from zero time to 7200 seconds. Generally speaking, the curves obtained with the probe in a horizontal position (Reiter and Sanford, 1973) are similar to those obtained in a vertical position (this report). The curves begin with a

VERTICAL THERMAL PROBE, UNCASED WELL - TEST RUNS NO. 52.48.45.39

FIRST DEGREE POLYNOMIAL FIT OF DATA

SPECIFIC DISCHARGE FOR #52 = 1; CM/DAY (⊙)

SPECIFIC DISCHARGE FOR #48 = 117 " (△)

SPECIFIC DISCHARGE FOR #45 = 236 " (+)

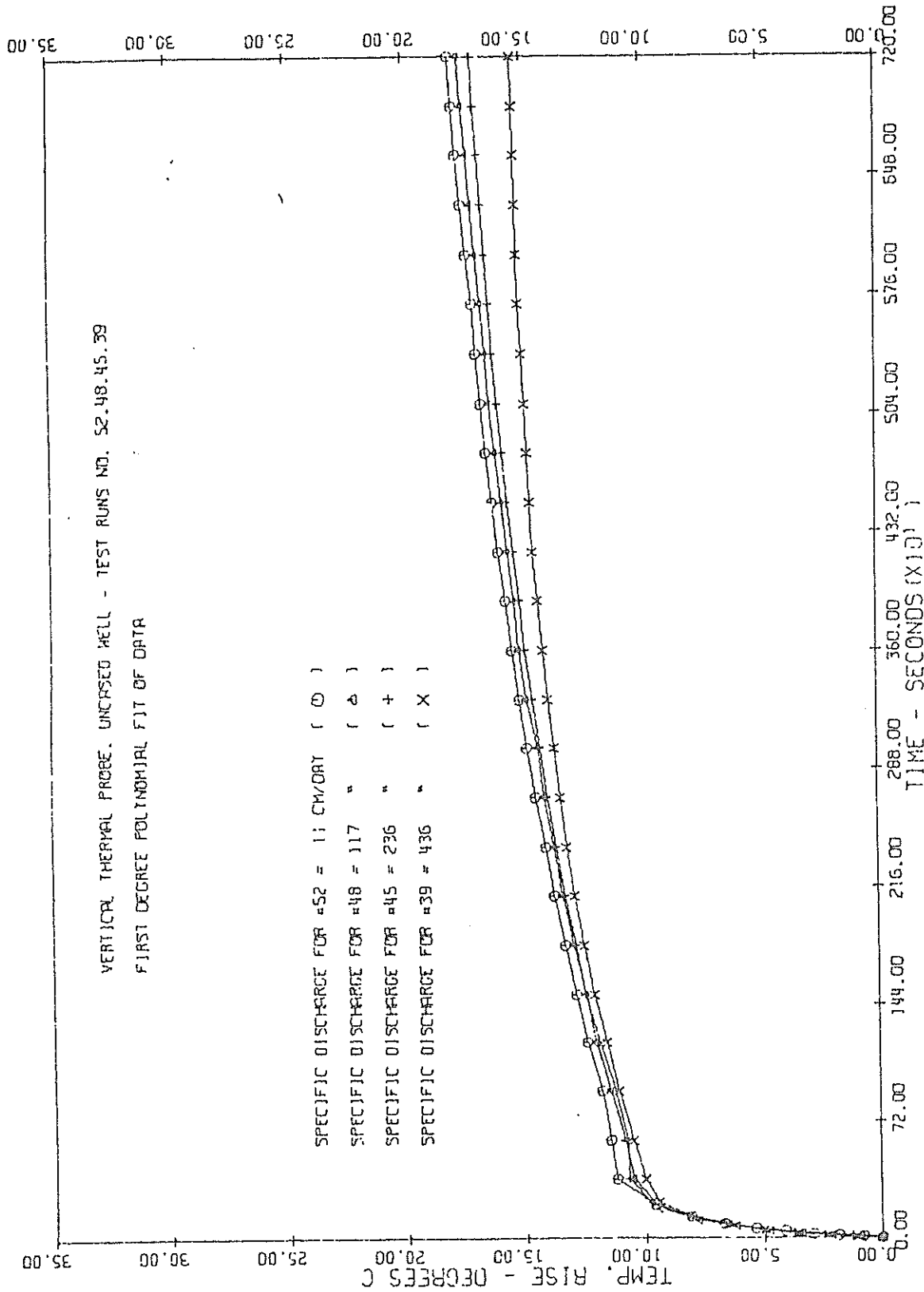SPECIFIC DISCHARGE FOR #39 = 436 " (X)

Figure 6   Some experimental curves for the rise in temperature of the thermal probe versus time (0 to 7200 seconds).

rapid, nearly linear rise in temperature. After about 200 seconds the rate of temperature increase is sharply reduced and there is a gradual decrease in the rate of temperature increase up to the end of each experiment. In Figure 6 the separation of curves for different water flow rates is small and sometimes reversed. Thus a plot of the entire data range for the various calibration tests does not yield a family of curves that is reliable in determining the water flow rates.

The sharp change in the character of the curves at about 200 seconds is caused by the onset of convection in the water surrounding the probe. Prior to this time the temperature gradient between the probe and the well screen is too small to sustain convection. Thus heat is initially transferred away from the probe by conduction. As the probe warms with increasing time, gradients become sufficiently large to support convection. Once this convection begins, heat is transferred more rapidly from the probe. Consequently, the rate of increase in the probe temperature is sharply reduced.

Calibration Curves

More than 58 calibration tests were performed; however, the first 22 were eliminated because of experimental errors in determining the specific discharge. Of the remaining 36 tests, 14 were used to establish master calibration curves for determining the specific discharge in a screened borehole. These 14 experimental runs were tests 29, 30, 31, 33, 38, 39, 40, 43, 44, 47, 48, 51, 52, and 56. These runs of two hours duration were conducted under the experimental procedures outlined at the end of the previous section.

As a first step in establishing master calibration curves, we obtained the best third order polynomial fit, in the least squares sense, for each of the 36 experimental runs. Coefficients for these polynomial fits are given in Table 2. Curve fitting was only applied to that portion of the experimental data from time equal to 1200 seconds to 7200 seconds. Consequently,

TABLE 1: Data for calibration runs: Screened borehole

st No.	Date	q(cm/day)	H(cm)	ST°C	ET°C	RT°C	MAX T°C
23	7-19-74	498	8.2	24.2	24.4	24.9	1.72
24	7-20-74	472	7.8	24.1	24.2	23.3	2.14
25	7-22-74	472	7.8	24.1	24.1	23.1	2.25
26	7-23-74	467	7.6	24.7	24.8	27.2	2.46
27	7-25-74	453	7.3	25.1	25.1	24.1	2.24
28	7-26-74	462	7.4	25.4	25.4	25.0	2.34
29	7-30-74	0	0	25.4	25.4	23.6	5.47
30	8-5-74	0	0	23.4	23.4	22.2	5.51
31	8-6-74	0	0	23.6	23.6	22.6	5.54
32	8-14-74	471	7.9	23.4	23.5	23.2	2.68
33	8-14-74	473	7.9	23.7	23.8	27.8	2.93
34	8-15-74	475	7.9	23.8	23.8	22.9	2.74
35	8-16-74	469	7.8	23.8	23.8	23.4	2.83
36	8-19-74	447	7.5	23.4	23.5	22.3	3.13
37	8-20-74	442	7.4	23.6	23.6	22.4	3.36
38	8-20-74	442	7.4	23.6	23.7	24.1	3.71
39	8-21-74	436	7.4	23.0	23.0	20.5	3.77
40	8-22-74	287	4.9	22.6	22.6	24.1	4.63
41	8-23-74	284	4.9	22.2	22.1	10.9	4.68
42	8-23-74	284	4.9	22.2	22.3	23.0	4.50
43	8-27-74	230	4.0	21.8	21.9	20.6	5.24
44	8-28-74	229	4.0	21.7	21.8	21.5	5.15
45	8-29-74	236	4.1	21.9	22.0	21.8	5.18
46	8-30-74	236	4.1	21.8	21.8	20.3	5.27
47	9-5-74	136	2.4	21.1	21.1	20.3	5.64
48	9-9-74	117	2.0	22.5	22.6	25.6	5.58
49	9-10-74	118	2.0	22.7	22.7	22.2	5.66
50	9-12-74	118	2.0	22.9	22.9	21.6	5.77
51	9-13-74	116	2.0	22.2	22.3	20.3	5.52
52	9-17-74	11	0.2	20.0	20.0	20.6	5.64
53	9-19-74	10	0.2	19.1	19.1	18.5	5.69
54	9-23-74	0	0	18.3	18.4	20.1	5.53
55	9-24-74	0	0	18.6	18.6	20.6	5.51
56	10-31-74	222	4.1	19.5	19.6	21.3	5.34
57	11-1-74	210	3.9	19.3	19.4	22.9	5.48
58	11-4-74	0	0	19.0	19.1	22.8	5.58

TABLE 2:   Coefficients from polynomial curve fitting

Test No.	A_o	$A_1 (\times 10^{-3})$	$A_2 (\times 10^{-7})$	$A_3 (\times 10^{-11})$
23	−1.415	1.506	−2.44	1.33
24	−1.746	1.830	−3.02	1.71
25	−1.862	1.973	−3.30	1.90
26	−1.813	1.866	−2.95	1.66
27	−1.812	1.925	−3.17	1.79
28	−1.889	1.976	−3.23	1.81
29	−2.227	2.131	−2.14	0.92
30	−2.216	2.135	−2.21	1.03
31	−2.278	2.200	−2.38	1.16
32	−1.973	1.910	−2.78	1.42
33	−2.036	2.107	−3.31	1.87
34	−1.868	1.901	−2.78	1.44
35	−1.943	2.020	−3.07	1.65
36	−2.006	2.005	−2.78	1.38
37	−2.095	2.069	−2.82	1.39
38	−2.135	2.150	−2.94	1.51
39	−2.166	2.163	−2.85	1.38
40	−2.286	2.182	−2.54	1.18
41	−2.282	2.218	−2.65	1.27
42	−2.051	2.029	−2.30	1.04
43	−2.234	2.177	−2.37	1.10
44	−2.215	2.116	−2.23	0.99
45	−2.262	2.208	−2.50	1.22
46	−2.337	2.297	−2.67	1.34
47	−2.265	2.199	−2.37	1.18
48	−2.327	2.185	−2.31	1.12
49	−2.386	2.273	−2.43	1.16
50	−2.085	1.973	−1.69	1.06
51	−2.321	2.193	−2.36	1.17
52	−2.281	2.153	−2.22	1.66
53	−2.147	2.030	−1.88	0.80
54	−2.088	2.001	−2.01	0.99
55	−2.118	2.008	−2.02	0.98
56	−2.256	2.167	−2.52	1.37
57	−2.144	2.062	−1.98	0.82
58	−2.182	2.092	−2.06	0.91

TABLE 3:   Description of headings listed in Tables 1 and 2

Heading

Test No.	Sequential number of test.
Date	Date that the test was performed.
q	Specific discharge in cm/day.
H	Difference in the levels of water between the upstream and downstream reservoirs on the calibration tank.
ST°C	The temperature of the water at the start of a test in degrees Centigrade.
ET°C	The temperature of the water at the end of a test in degrees Centigrade.
RT°C	The room temperature half way through a test in degrees Centigrade.
MAXT°C	The maximum temperature rise in the probe using the probe temperature at 1200 seconds as zero, in degrees Centigrade.
A_o	Constant coefficient from third order polynomial fit of data.
A_1	First order coefficient from the data fit; each value in the table is multiplied by 10^{-3}.
A_2	Second order coefficient from the data fit; each value in the table is multiplied by 10^{-7}.
A_3	Third order coefficient from the data fit; each value in the table is multiplied by 10^{-11}.

the temperature rise was with respect to the observed temperature at 1200

seconds; that is, 1200 seconds was taken as the new origin. This technique

provided better curve separation for the various flow rates.

The A_0 coefficients of the polynomial fits are intercept values and ap-

pear to depend on the temperature at which convection begins. Because the

initial temperature contrast between the probe and the water ranged up to

2°C in the tests, no correlation between A_0 values and flow rates is to be

expected in the data listed in Table 2.

A preliminary examination of the A_1 coefficients for the 36 tests seemed

to indicate a fairly constant value for most of the tests. For those values

of the A_1 coefficient that are 2.00×10^{-3} or higher (27 tests in all),a mean

value is 2.13×10^{-3} with a standard deviation of 0.08×10^{-3}. This gives

a range of A_1 values from 2.05×10^{-3} to 2.21×10^{-3} that are within one

standard deviation of the mean. There are 18 tests falling within this range

that have a new mean of 2.15×10^{-3} and a new standard deviation of 0.05×10^{-3}.

Thus a second refined range of values for the A_1 coefficients that are within

one standard deviation of the new mean is 2.10×10^{-3} to 2.20×10^{-3}. This

new range includes the 14 calibration tests, mentioned above, that were used

to construct the initial calibration curves. Similar procedures were used

to analyze the A_2 and A_3 coefficients. However, they do not appear to follow

any definite trend with changes in flow rates and no further use was made of

them.

Plots of temperature rise versus time for the 14 tests listed above

are shown in Figures 7, 8 and 9. From these curves it is apparent that

curve separation is too small to measure flow rates below about 120 cm/day.

Above this limiting value, curve separation is good and flow rates can be

determined from the thermal probe. Figure 10 is a plot of maximum temperature

rise recorded in the probe at 7200 seconds versus the specific discharge for the 14 tests. It provides a single master calibration curve from which the specific discharge can be read directly. At specific discharge rates below about 120 cm/day, the curve is nearly flat, and specific discharge cannot be determined accurately. Above this value, the specific discharge can be read from the graph directly. However, the number of data points is not sufficient to clearly define the curves over all specific discharges.

A close examination of Figures 7 and 8 does show some curve overlap. Improvement in the master curves can be obtained by eliminating those curves which over-lap (tests 44, 47 and 56) or have different values of maximum temperature rise for the same specfic discharge (tests 29, 30, 31 and 33). The remaining seven tests (numbers 38, 39, 40, 43, 48, 51, and 52) are used to construct the final calibration curves. In addition tests 41, 45, and 58 all have A_1 coefficients that are just outside the range used in the original test selection. These three tests show no curve overlap with other tests and their respective maximum temperature rises appear to follow the pattern of the remaining seven tests. Therefore, these three tests are also used in establishing the final calibration curves.

Plots of temperature rise versus time using the ten tests mentioned above are shown in Figures 11 and 12. Again, specific discharge rates below about 120 cm/day cannot be determined. However, above this rate there is excellent curve separation and specific discharge rates are apparently accurately determined. A plot of the maximum temperature rise in the probe versus specific discharge is shown in Figure 13. The curve is nearly horizontal for specific discharge rates between 0 and 120 cm/day, but is nearly linear at higher values of specific discharge. It thus appears that the thermal probe can measure specific discharge only when the rate is above 120 cm/day.
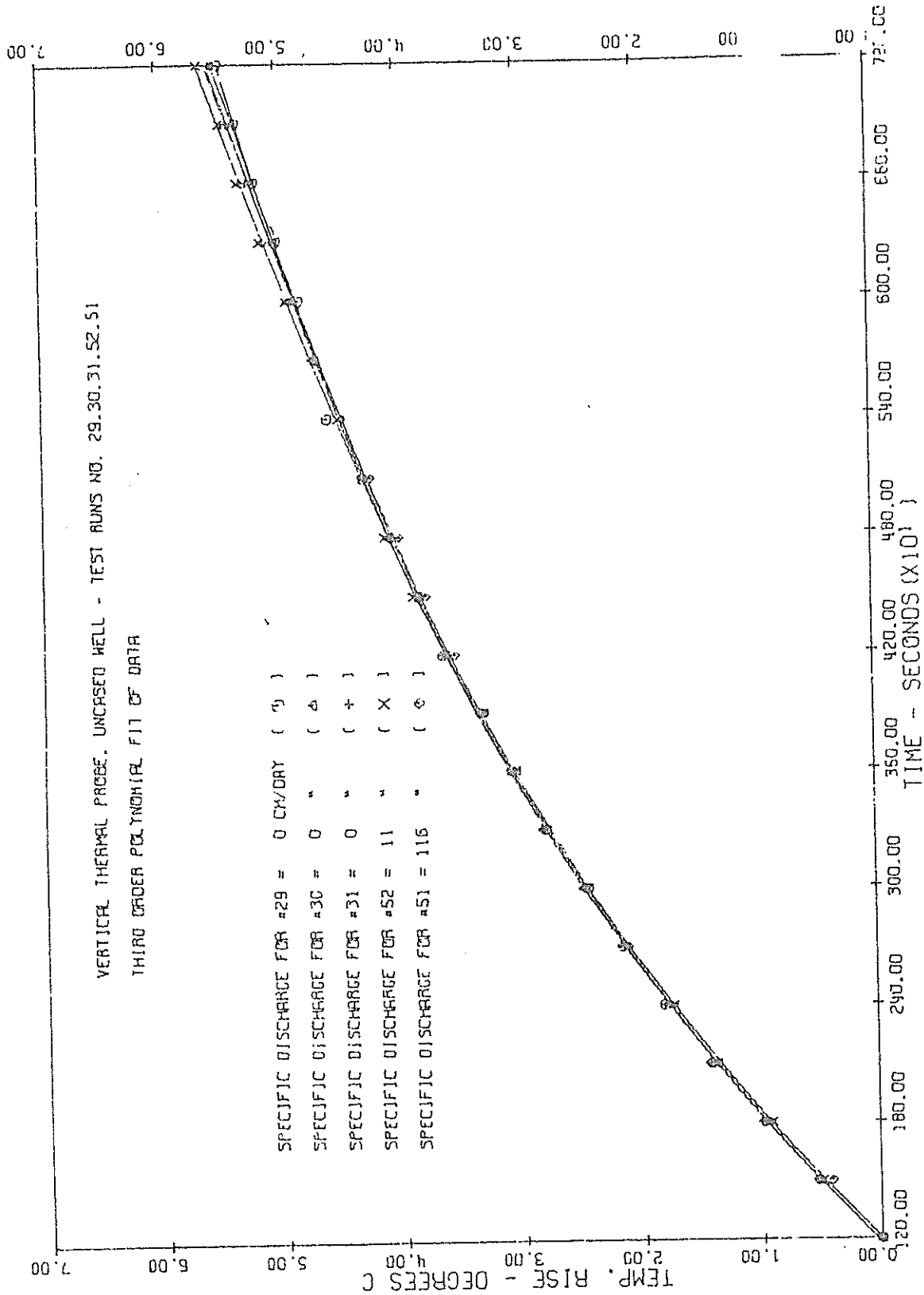
FIGURE 7 Experimental curves for the rise in temperature of the thermal probe versus time for specific discharges of 0 to 116 cm/day.
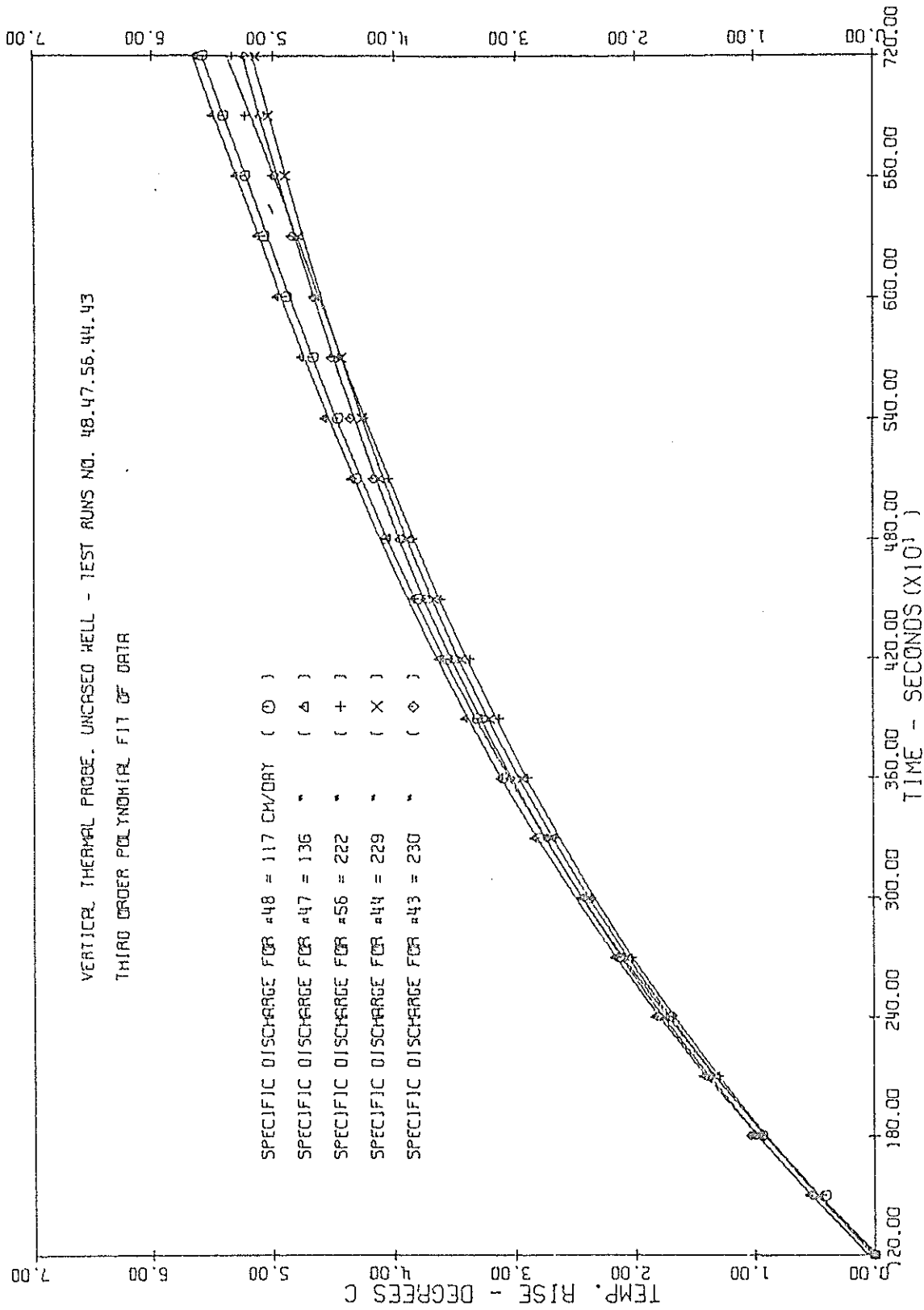
FIGURE 8 Experimental curves for the rise in temperature of the thermal probe versus time for specific discharges of 117 to 230 cm/day.
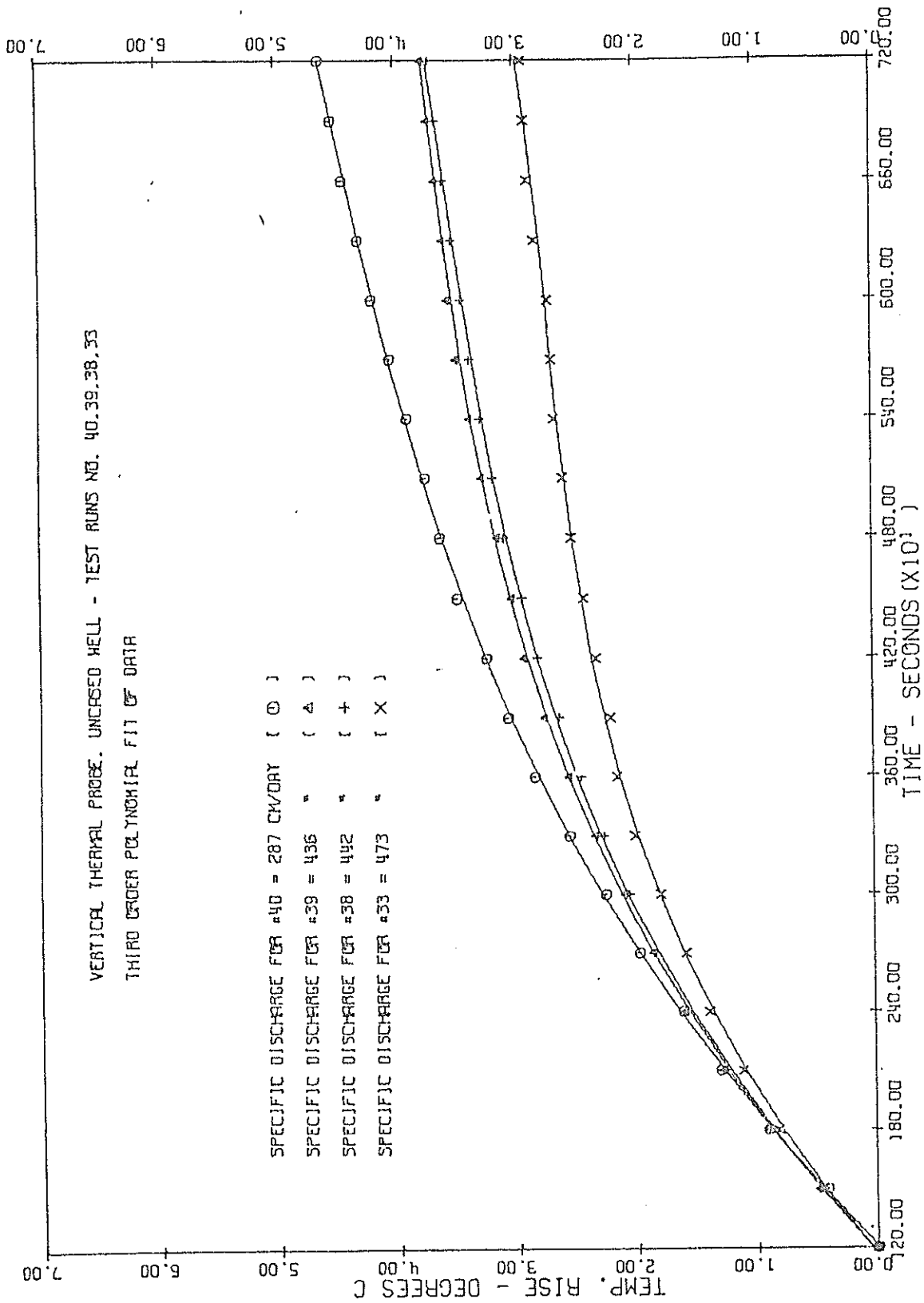
Figure 9 Experimental curves for the rise in temperature of the thermal probe versus time for specific discharges of 287 to 473 cm/day.
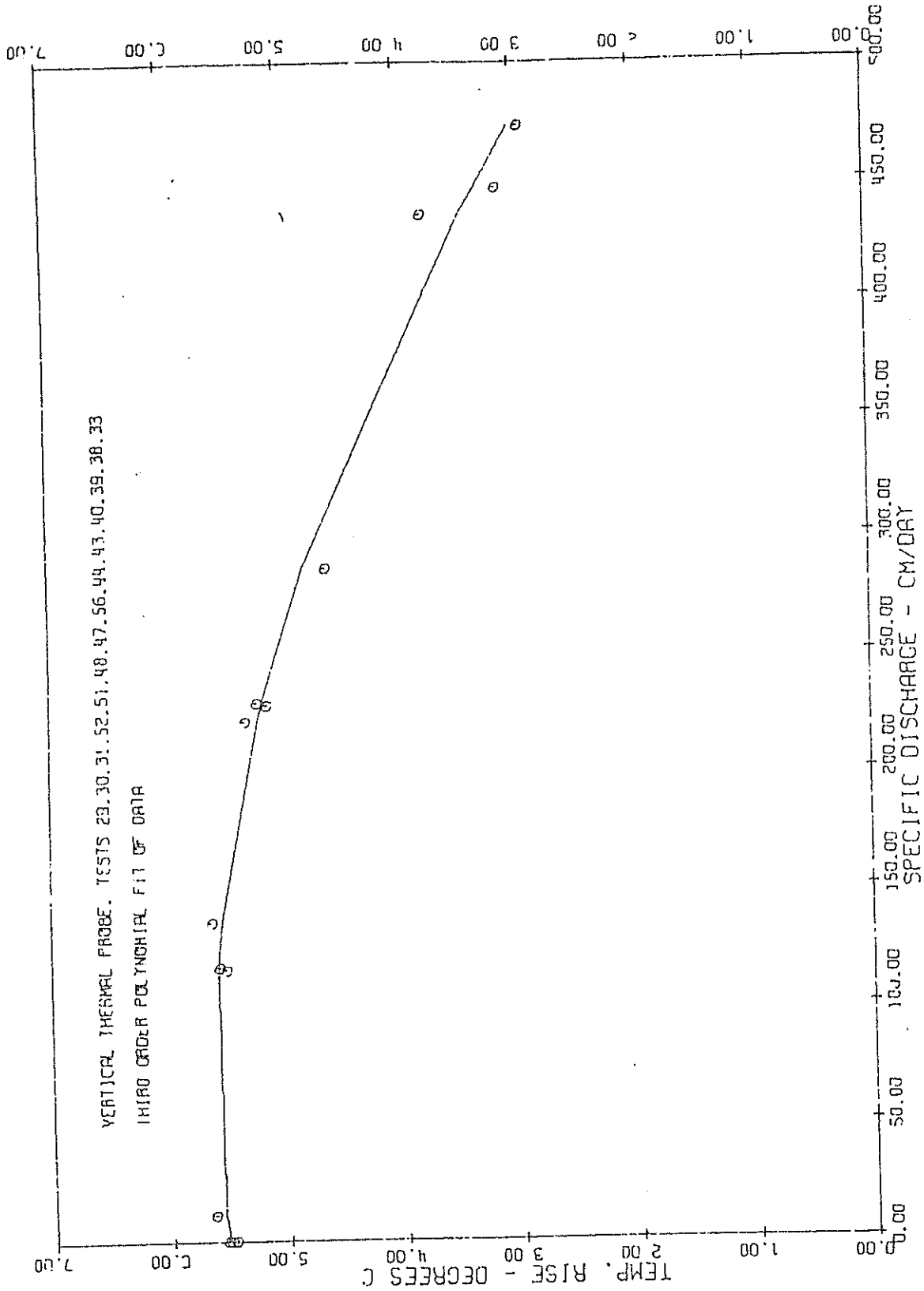
Figure 10   Curve showing the maximum temperature rise in the probe versus
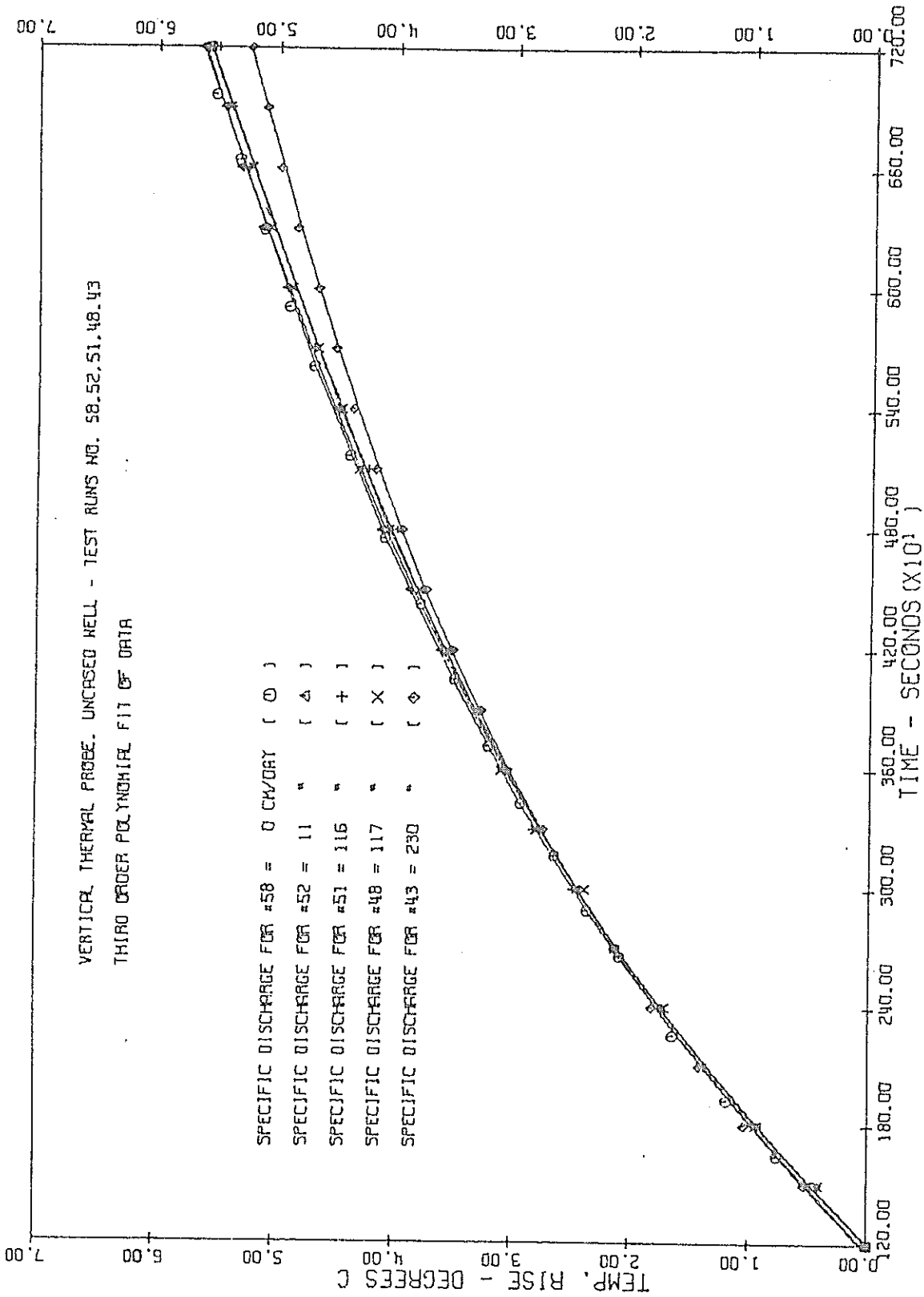specific discharge for tests shown in Figures 7, 8 and 9.

Figure 11 Experimental curves for the rise in temperature of the thermal probe versus time for specific discharges of 0 to 230 cm/day.
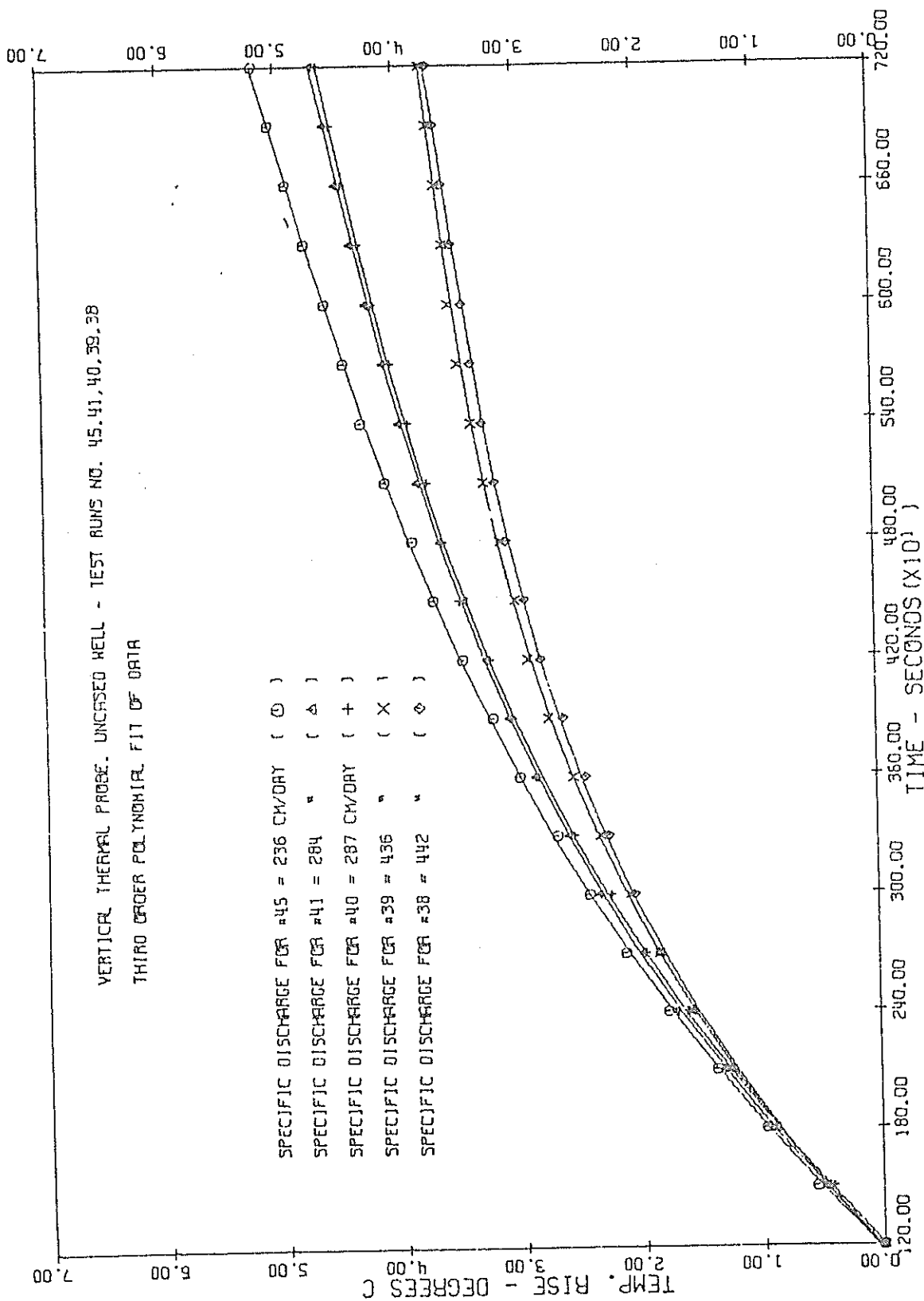
Figure 12 Experimental curves for the rise in temperature of the thermal probe versus time for specific discharges of 236 to 442 cm/day.
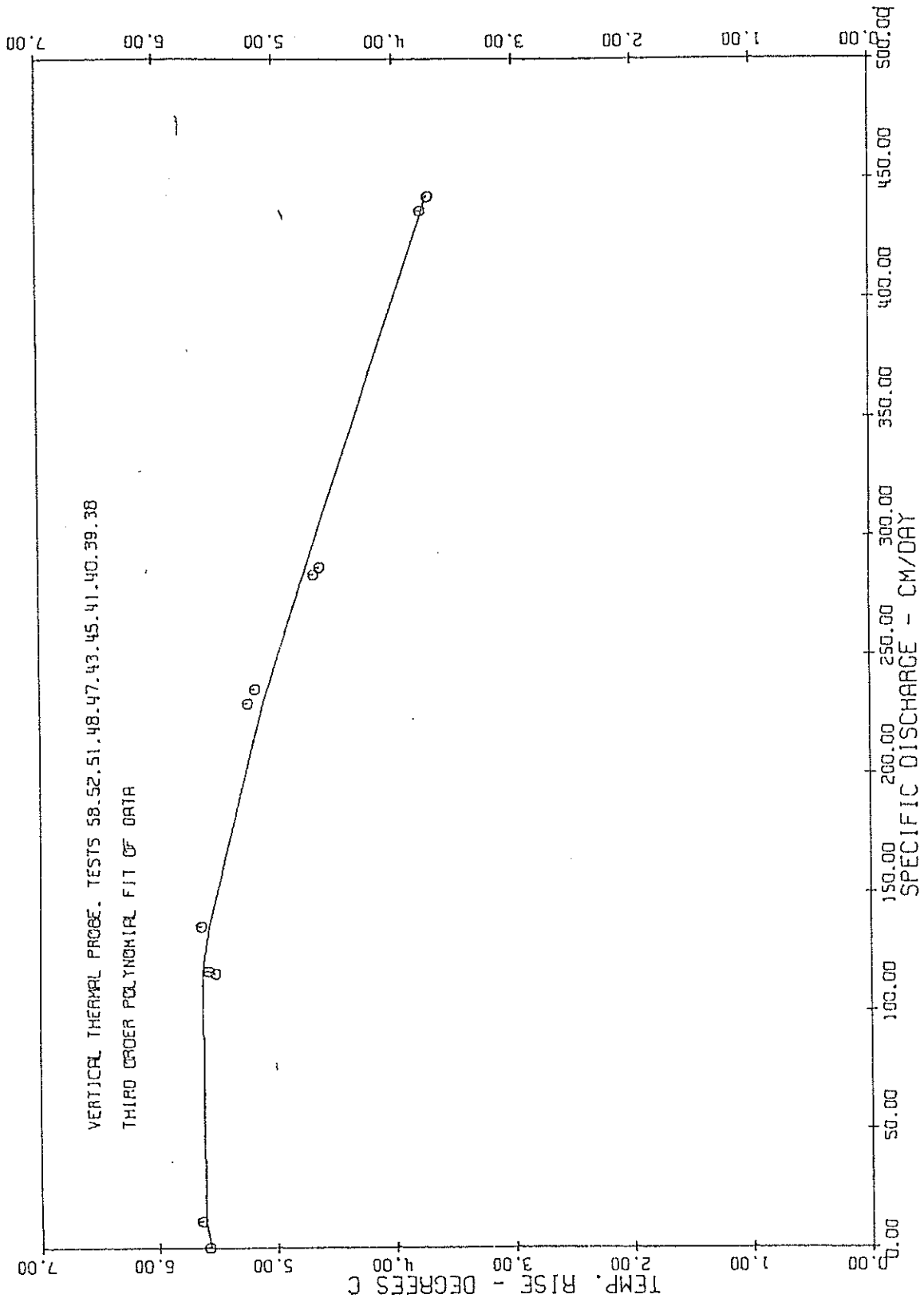
Figure 13 Curve showing the maximum temperature rise in the probe versus specific discharge for tests shown in Figures 11 and 12.

SUMMARY AND CONCLUSIONS

The thermal probe described in this report was designed for the in-situ measurement of groundwater flow rates in the cased and screened portion of water wells. An accurate theoretical evaluation of the probe is difficult because of the complex interaction of the radial flow of heat away from the probe and the linear flow of water past the borehole. For this reason full scale calibration in the vertical position was performed in order to experimentally determine its sensitivity and useful range of measurement.

Basically, the probe is a long slender metal rod having a heat sensor at its midpoint. When a constant quantity of heat is applied to the probe, the rise in temperature is inversely related to the rate of water flowing past the borehole. Full scale calibration of the probe was achieved by using a large metal tank having a central sand-filled chamber with a well screen in its center to hold the probe. The central chamber was hydrologically connected to upstream and downstream water reservoirs. These reservoirs were used to control the rate of water flowing in the sand, and thus past the borehole.

Fifty-eight calibrations of the thermal probe were made at various flow rates, but most of these were used to perfect experimental techniques. Much of the data overlapped and were of questionable value because of the various experimental problems and test procedures involved. However, ten experimental curves which follow the expected sequence for the corresponding changes in specific discharge were obtained. By fitting a third order polynomial to these ten best experimental curves, a set of master calibration curves was obtained for the thermal probe (Figures 11 and 12). The polynomial fitting smoothed out the experimental data and allowed each predicted calibration curve to be based upon the best available data. The calibration

curves obtained in this study indicate that if temperature differences on the order of 0.1°C can be experimentally measured after two hours, the probe is sensitive enough to distinguish specific discharge rates as low as 0.0014 $cm^3/sec/cm^2$ (120 cm/day).

An important source of error in the calibration of the probe was the inability to maintain a constant temperature throughout the tank. Because of diurnal variations in the room temperature and the slow movement of water through the sand, the temperature of the water flowing past the probe would characteristically show a 0.5°C cyclical change in 24 hours. In the two hour calibration tests, the change in temperature of water flowing passed the probe probably never exceeded 0.1°C, but this change may have been adequate to account for overlap of some of the calibration curves. However, temperature fluctuations of ±0.1°C within the tank do not change the basic conclusion of this study that flow rates below 120 cm/day cannot be measured.

REFERENCES CITED

Jaeger, J. C., 1940, "Radial Heat Flow in Circular Cylinders with General Boundary Conditon I", Jour. Roy. Soc. N.S.W., Vol. 74, pp. 342-352.

_____, 1956, "Conduction of Heat in Infinite Region Bounded Internally by a Circular Cylinder of a Perfect Conductor", Aust. Jour. Phys., Vol. 9, pp. 167-197.

Reiter, M. A., and Sanford A. R., 1973, "Measurement of Groundwater Flow using an In-Situ Thermal Probe", New Mexico Water Resources Research Institute Report No. 027, New Mexico State University, Las Cruces, 31 p.